Available online at www.sciencedirect.com
ScienceDirect
Nuclear Instruments and Methods in Physics Research B 260 (2007) 124–129
NIM B
Beam Interactions with Materials & Atoms
www.elsevier.com/locate/nimb

Nano-imaging of single cells using STIM

Ren Minqin [a,b], J.A. van Kan [a], A.A. Bettiol [a], Lim Daina [c], Chan Yee Gek [c], Bay Boon Huat [c], H.J. Whitlow [d], T. Osipowicz [a], F. Watt [a,*]

[a] Centre for Ion Beam Applications (CIBA), Department of Physics, National University of Singapore, Singapore 117542, Singapore
[b] Department of Biochemistry, National University of Singapore, Singapore
[c] Department of Anatomy, National University of Singapore, Singapore
[d] Department of Physics, University of Jyvaskyla, P.O. Box 35 (YFL), FIN-40014, Finland

Available online 14 February 2007

Abstract

Scanning transmission ion microscopy (STIM) is a technique which utilizes the energy loss of high energy (MeV) ions passing through a sample to provide structural images. In this paper, we have successfully demonstrated STIM imaging of single cells at the nano-level using the high resolution capability of the proton beam writing facility at the Centre for Ion Beam Applications, National University of Singapore. MCF-7 breast cancer cells (American Type Culture Collection [ATCC]) were seeded on to silicon nitride windows, backed by a Hamamatsu pin diode acting as a particle detector. A reasonable contrast was obtained using 1 MeV protons and excellent contrast obtained using 1 MeV alpha particles. In a further experiment, nano-STIM was also demonstrated using cells seeded on to the pin diode directly, and high quality nano-STIM images showing the nucleus and multiple nucleoli were extracted before the detector was significantly damaged.

PACS: 78.70.−g; 82.80.Yc; 87.64.−t

Keywords: Nano-imaging; Nano-STIM; STIM; Scanning transmission ion microscopy; Single cell imaging; Nuclear microscopy

1. Introduction

There has recently been an upsurge in interest into new methods of imaging biological cells and tissue. Scanning transmission ion microscopy (STIM) which was demonstrated over 20 years ago [1] has the potential for producing structural images of cells and tissue, but has been infrequently utilised by only a few nuclear microprobe groups over the last two decades. STIM relies on measuring the energy loss of a beam of highly focused MeV ions as it passes through a sample, and because the transmitted protons in general maintain a straight path as they pass through a biological specimen (e.g. a tissue section or a cell), then a high quality structural image of a relatively thick specimen can be formed. The use of STIM has in general been limited to identifying specific regions of interest in a biological sample prior to elemental analysis by nuclear microscopy [2–14], but has also been used to construct tomographic structural images of specimens that are difficult to section [15–19].

Recently it has been possible to focus an MeV proton beam to below 100 nm, achieved in the proton beam writing facility of the Centre for Ion Beam Applications (CIBA), National University of Singapore [20]. The p-beam writing facility uses OM52 lenses arranged in a compact couplet triplet formation resulting in increased X and Y demagnifications of 228×60, respectively. Sub-100-nm beams are routine, with a current achievable best spot size of 35×75 nm for 10 000 protons per second [20]. The use of high energy ion beams focused to nano-dimensions raises the possibility of STIM nano-imaging of single cells and tissue. Since this resolution is well below the wavelength of light and is maintained through relatively

* Corresponding author. Tel.: +65 65162815; fax: +65 67776126.
E-mail address: phywattf@nus.edu.sg (F. Watt).

0168-583X/$ - see front matter © 2007 Elsevier B.V. All rights reserved.
doi:10.1016/j.nimb.2007.02.015

thick tissue sections and whole cells, the nano-STIM technique could well have significant potential for structural imaging in biomedicine.

2. Experimental details

The CIBA proton beam writing line, which can routinely focus MeV ion beam to sub-100 nm dimensions, is not readily amenable for either STIM or nuclear microscopy investigations, since the target stage to lens distance is reduced to 7 cm compared to 15 cm in the CIBA nuclear microscopy line [20]. To adapt to the reduced working distance we have constructed a miniature assembly using a Hamamatsu pin diode S1223-01 (3.06×3.06 mm chip) [21] mounted in a miniature assembly fronted by a silicon nitride window of thickness 50 nm (see Fig. 1). The cells (MCF-7 American Type Culture Collection [ATCC] breast cancer cells) were successfully grown on the upper surface of the silicon nitride window, as indicated by the optical micrograph of the cells on the silicon nitride window shown in Fig. 2. The cells were prepared according to the protocol as described in Table 1, which is a procedure used in cell biology, to preserve the structural integrity of the cells. The STIM assembly was mounted on a computer-controlled Burleigh Inchworm EXFO XYZ stage which has a travel of 25 mm for all axes with a 20 nm closed loop resolution [22].

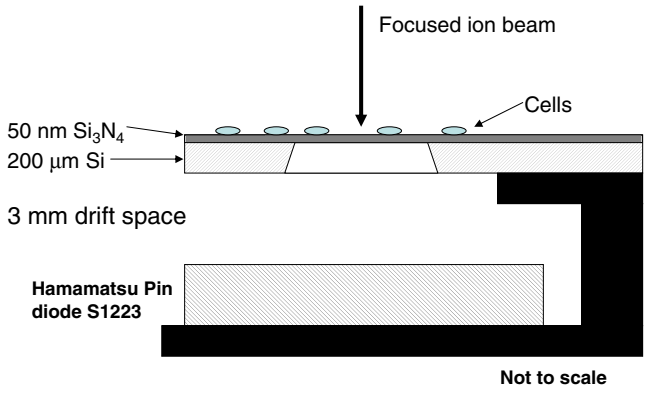

Fig. 1. Schematic diagram of the STIM assembly, showing the silicon nitride window and the pin diode. The cells are grown on the upper surface of the silicon nitride window.

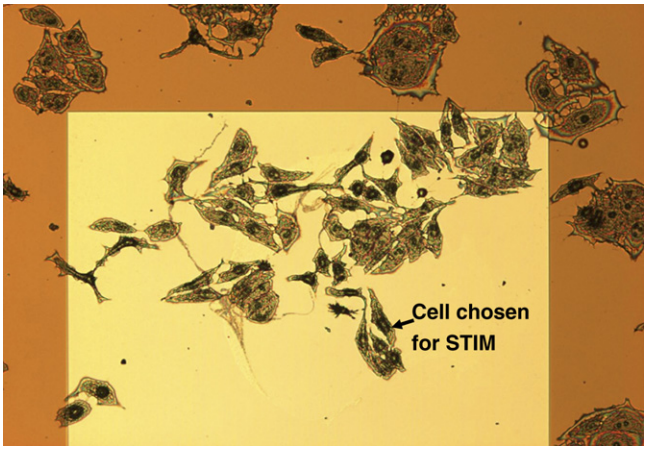

Fig. 2. Optical micrograph of the breast cancer cells grown on a 50 nm thick silicon nitride window (500 μm × 500 μm). The cell chosen for the STIM studies is marked in the figure.

3. Results and discussion

3.1. Results of STIM using the silicon nitride window as substrate

A 2 MeV H_2^+ beam (an H_2^+ ion is equivalent to two 1 MeV protons) was focused down to sub 100 nm, and scanned across a suitable cell located on the silicon nitride window as shown in Fig. 2. A H_2^+ beam rather than a 1 MeV proton beam was chosen because this represents the brightest beam from the accelerator, and also because the beam halo due to slit scattering is minimized (the H_2^+ beam splits into two protons on contact with the slit edges and therefore have a very different focal point). A one MeV alpha beam was also focused to sub-100 nm and scanned across the same cell. The STIM spectra from the cell for both the H_2^+ and the alpha beam were collected by the Hamamatsu pin diode positioned directly behind the window and operating at a 10 V bias voltage. It can be seen from the STIM energy spectra shown in Fig. 3 that the H_2^+ STIM energy spectrum displays relatively little energy loss compared with the alpha beam, expected because of the higher stopping power of the 1 MeV alpha particles compared with the 1 MeV protons (408 keV/μm for alpha particles and 52 keV/μm for protons in carbon). The energy resolution of the Hamamatsu pin diode, chosen at random from a batch purchased from the manufacturer, was measured to be 23 keV for the 1 MeV alpha particles and around 27 keV for the 2 MeV H_2^+. Estimates of the straggling of the protons and alpha beam traversing the 50 nm substrate window (1 keV for 1 MeV protons and 2.4 keV for 1 MeV alpha particles) as calculated by SRIM [23] were small compared with the detector energy resolution. The STIM images for both the H_2^+ and alpha beam were collected using the OMDAQ system [24] using a median energy fit, and are shown in Fig. 4. As expected, the STIM image using the alpha beam exhibits a higher contrast compared with the image using the H_2^+ beam, although in both cases the cell nucleus is clearly visible.

3.2. Results of STIM using the pin diode as substrate

In a second experiment, it was decided to investigate STIM imaging using the pin diode as substrate, thereby dispensing with the relatively fragile silicon nitride window. Two potential problems were investigated: (a) growing the cells on the pin diode and (b) damage incurred by the pin diode due to the incoming ion beam. As shown in Fig. 5, growing the cells on the pin diode by following the same

Table 1
Cell preparation protocol

Culturing of the breast cancer cells: MCF-7 breast cancer cells (American Type Culture Collection [ATCC HTB-22]) were maintained in Dulbecco's modified Eagle Medium (DMEM, Sigma) supplemented with 10% fetal bovine serum (FBS, Hyclone) at 37 °C in a humidified atmosphere (95% air and 5% CO_2). Cells were harvested by trypsin treatment and seeded on the SiN substrate.
Processing of cultured cells: The silicon nitride window was first UV sterilized (30 min) and the cells plated on to the window. The culture medium was removed and the cells given a quick wash with phosphate buffer (PB) (0.1 M pH 7.4). Cells were then fixed with 3% Glutaraldehyde (prepared in 0.1 M PB pH 7.4) for 1 h. The fixative was then removed and cells washed with PB for 5 min (3×). The cells were then passed through a series of ethanol: 25% – 3 min, 50% – 3 min, 75% – 3 min, 95% – 3 min, 100% – 5 min, 100% – 5 min.
Critical point drying: The samples were then transferred into the critical point dryer (BAL-TEC CPD 030) and dried after about 1 h. (Samples were placed in small porous containers to ensure they were not damaged during the drying process.) The pressure was released slowly after drying to avoid rupturing the 50 nm silicon nitride window.

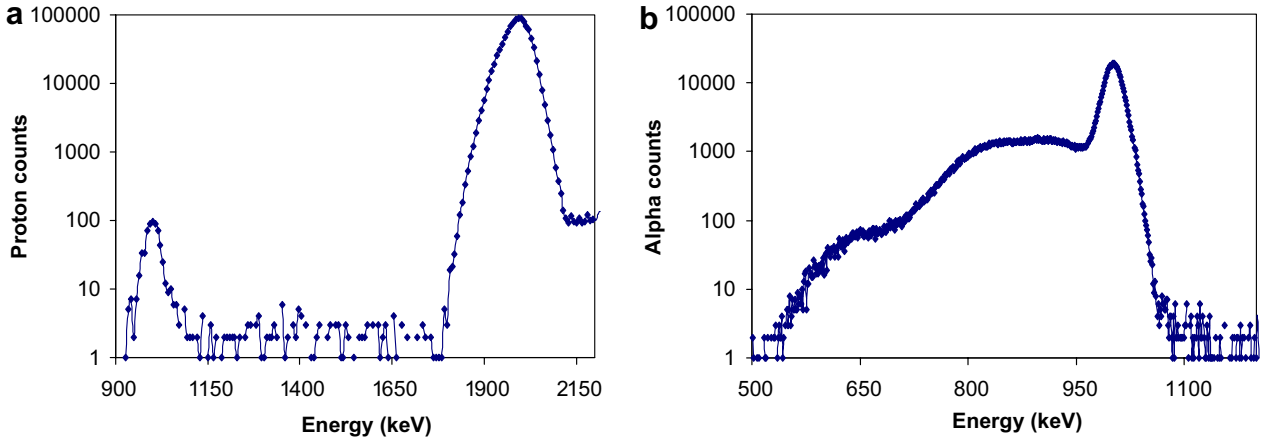

Fig. 3. STIM energy spectra from (a) 2 MeV H_2^+ beam scanning over the cell depicted in Fig. 2, and (b) 1 MeV alpha beam scanning over the same cell.

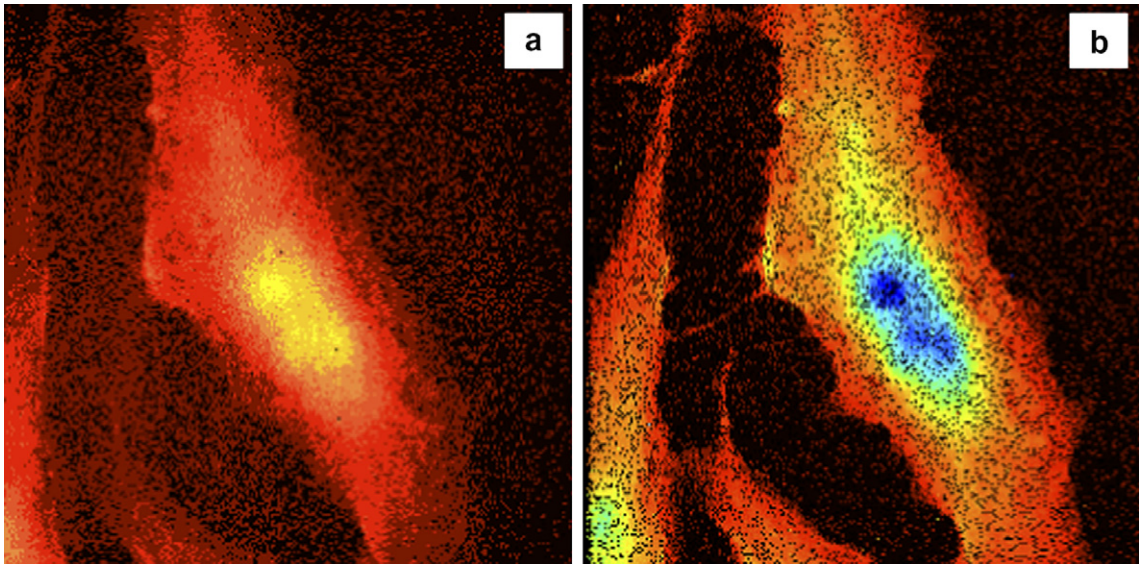

Fig. 4. STIM images of the cell on the silicon nitride window as depicted in Fig. 2, using (a) 2 MeV H_2^+ beam and (b) 1 MeV alpha beam. The scan size is 40 μm in each case and the STIM images have been assembled using a median energy fit.

protocol as described in Table 1 proved remarkably successful, provided that the pin diode was pre-sterilised using UV radiation. The question of damage to the pin diode is addressed in the next section. Fig. 6 shows the images of proton and alpha STIM of two different cells grown on the pin diode. As expected, once again the alpha STIM

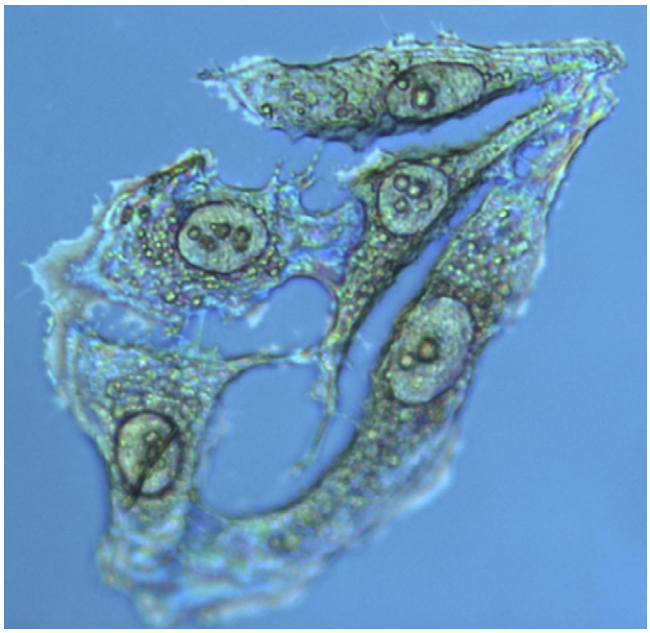

Fig. 5. Optical micrograph of breast cancer cells plated on the pin diode surface, showing a high degree of structural integrity.

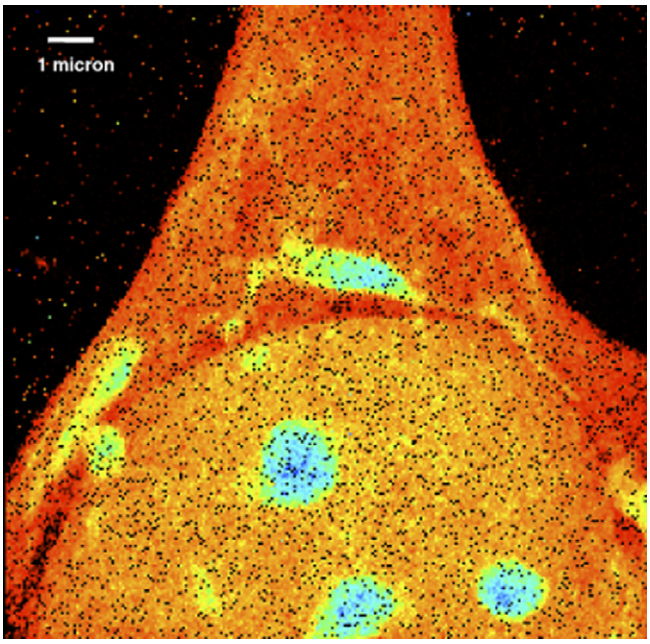

Fig. 7. An alpha STIM image of a cell grown directly on the pin diode (as depicted in Fig. 6(b)). The scan size is 15 μm and the STIM image has been assembled using a median energy fit. The beam size is 80×90 nm.

exhibited more contrast than the proton STIM. As a further test of nano-STIM, a 1 MeV alpha beam was focused down to 80×90 nm (as measured by the new CIBA resolution standard [25], both before and after the scan), and scanned over the same cell depicted in Fig. 6(b) with a reduced scan size of 15×15 μm. Each pixel in the 256×256 image is therefore 60×60 nm, and therefore slightly smaller than the beam spot size. The high magnification STIM image is shown in Fig. 7 and the nucleus together with multiple nucleoli are clearly observed.

3.3. Results of the beam damage incurred using the pin diode as substrate

The contrast of the STIM image of the cells plated directly on to the pin diode is ultimately dependent on the damage incurred by the pin diode due to the incoming ions. As the ion beam interacts with the depletion layer of the diode, damage results in the formation of trapping centres which in turn reduces the charge induced by single ions. Detailed information about the precise effects and generating mechanisms of this damage build-up can be

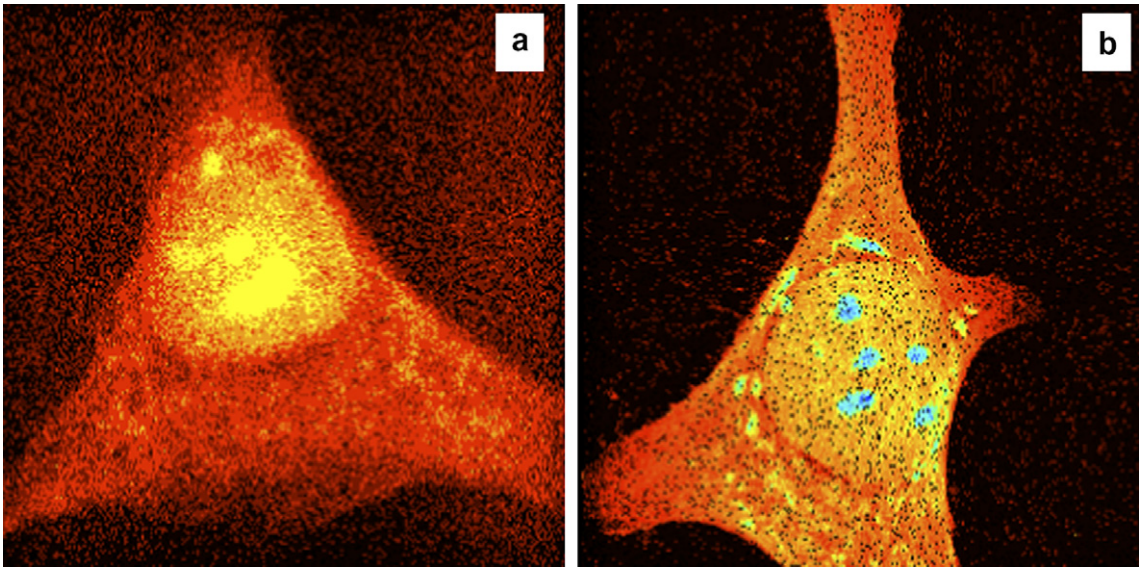

Fig. 6. STIM images of cells grown directly on the pin diode, using (a) 2 MeV H_2^+ beam and (b) 1 MeV alpha beam. The scan size is 40 μm in each case and the STIM images have been assembled using a median energy fit.

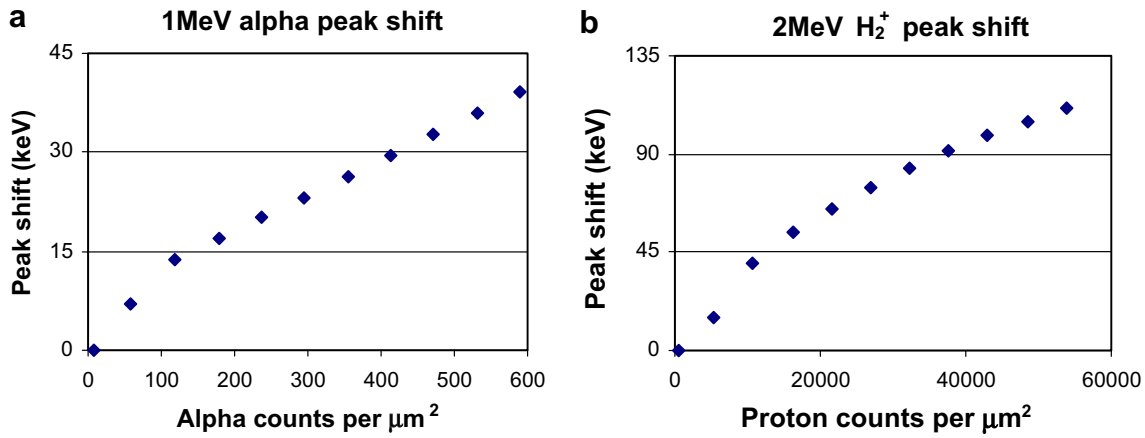

Fig. 8. Peak energy shift caused by ion beam damage on a pin diode from (a) 1 MeV alpha particles, and (b) 1 MeV protons (2 MeV H_2^+).

found in [26–29]. In general, we require the STIM image to be formed before the induced charge is reduced by an amount approximately equal to the energy resolution of the detector. To investigate the damage caused by the 1 MeV proton and alpha beam, two untouched regions of a pin diode were selected. Each region (40×40 μm) was scanned using 1 MeV protons (2 MeV H_2^+) and 1 MeV alphas, and the data were recorded in list mode files. Fig. 8 shows the results of these measurements: the position of the peak was extracted sequentially from the list mode files, and is plotted as a function of the number of ions per μm^2. As expected, the initial shift in energy due to damage created by the alpha beam (6.1 keV/100 ions/μm^2 = 6.1 keV/10^{10} ions/cm^2) is higher than that from the protons (0.35 keV/100 ions/μm^2 = 0.35 keV/10^{10} ions/cm^2), and these results are in reasonable agreement with measurements reported earlier [30,31]. Since a typical STIM image would contain on average around 10 counts per pixel, and for nano-STIM a pixel size corresponding to 50 nm is currently feasible, then the requirements of 4000 counts per μm^2 without incurring significant detector damage is just about possible for proton STIM. For alpha STIM, although there is increased detector damage, this increased damage is not so critical since the energy loss of the alpha particles transmitted through a biological cell is also increased (see Fig. 3). Nevertheless, to obtain the maximum contrast for the alpha nano-STIM images we may need a correction procedure to account for the accumulated damage if we use resolutions significantly better than 100 nm.

4. Conclusion

Structural imaging at the nanoscale using either MeV protons or alpha particles is now possible. The proton beam writing facility at the Centre for Ion Beam Applications, National University of Singapore, has been used in these studies and because of the limited space available a small STIM assembly has been constructed utilizing a 50 nm silicon nitride window backed by a Hamamatsu pin diode acting as particle detector. The nano-STIM technique has been demonstrated successfully using breast cancer cells (MCF-7 American Type Culture Collection [ATCC]) attached to the silicon nitride windows. A reasonable contrast was obtained using 1 MeV protons and an excellent contrast obtained using higher stopping power 1 MeV alpha particles. In a further experiment, nano-STIM was also demonstrated using cells attached to the pin diode directly, and high quality STIM images were extracted before the detector was significantly damaged. The nano-STIM technique has high potential in structural imaging of whole single cells, since the spatial resolution of the proton or alpha particle beam through the cell is maintained. The contrast is heavily influenced by the stopping power of the incident ion and the energy resolution of the STIM detector. Here we have used a Hamamatsu pin diode picked at random from a batch purchased from the manufacturer. If a higher resolution detector is used then the contrast will be higher and *vice versa*. It is unlikely that PIXE and RBS techniques can be used simultaneously with STIM using a pin diode as a substrate, since the increased beam current densities required for these techniques will lead to excessive detector damage. In such experiments the use of a thin SiN window as substrate and an off-axis STIM detector would be necessary. Other techniques such as direct nano-STIM correlated with low current ion beam fluorescence imaging may prove to have a high potential, since cellular fluorescence imaging at spatial resolutions well below the diffraction limit of light will then be possible. Although the present tests proved successful, the cells were dehydrated and therefore distorted. However, if flash frozen hydrated cells are used and analysed in the frozen state to avoid sublimation, it may be possible to extend the technique to 3D nano-STIM imaging.

References

[1] J.C. Overley, R.C. Connolly, G.E. Sieger, J.D. MacDonald, H.W. Lefevre, Nucl. Instr. and Meth. 218 (1983) 43.
[2] I. Guinote, R. Fleming, R. Silva, P. Filipe, J.N. Silva, A. Verıssimo, P. Napoleao, L.C. Alves, T. Pinheiro, Nucl. Instr. and Meth. B 249 (2006) 697.

[3] R. Ortega, Nucl. Instr. and Meth. B 231 (2005) 218.
[4] M. Wegden, P. Kristiansson, C. Ceberg, P. Munck af Rosenschold, V. Auzelyte, M. Elfman, K.G. Malmqvist, C. Nilsson, J. Pallon, A. Shariff, Nucl. Instr. and Meth. B 219–220 (2004) 67.
[5] M.Q. Ren, P.S.P. Thong, U. Kara, F. Watt, Nucl. Instr. and Meth. B 150 (1999) 179.
[6] Ph. Moretto, Y. Llabador, Nucl. Instr. and Meth. B 130 (1997) 324.
[7] F. Watt, Nucl. Instr. and Meth. B 130 (1997) 1.
[8] A.N. Hogarth, P.S.P. Thong, D.J.W. Lane, F. Watt, Nucl. Instr. and Meth. B 130 (1997) 402.
[9] Ph. Moretto, R. Ortega, Y. Llabador, M. Simonof, J. Benard, Nucl. Instr. and Meth. B 104 (1995) 292.
[10] M. Cholewa, G.J.F. Legge, H. Weigold, G. Holan, C. Birch, Nucl. Instr. and Meth. B B77 (1993) 282.
[11] Ph. Moretto, Y. Llabador, R. Ortega, M. Simonoff, L. Razafindrabe, Ph. Moretto, Y. Llabador, R. Ortega, M. Simonoff, L. Razafindrabe, Nucl. Instr. and Meth. B75 (1993) 511.
[12] F. Watt, J.P. Landsberg, Nucl. Instr. and Meth. B 77 (1993) 249.
[13] M.B.H. Breese, J.P. Landsberg, P.J.C. King, G.W. Grime, F. Watt, Nucl. Instr. and Meth. B 64 (1992) 505.
[14] J.P. Landsberg, B. McDonald, F. Watt, Nature 360 (1992) 65.
[15] M. Schwertner, A. Sakellariou, T. Reinert, T. Butz, Ultramicroscopy 106 (2006) 574.
[16] C. Michelet, Ph. Moretto, Nucl. Instr. and Meth. B 158 (1999) 361.
[17] R. Ortega, G. Deves, Ph. Moretto, Nucl. Instr. and Meth. B 181 (2001) 475.
[18] C. Habchi, D.T. Nguyen, G. Deves, S. Incerti, L. Lemelle, P. Le Van Vang, Ph. Moretto, R. Ortega, H. Seznec, A. Sakellariou, C. Sergeant, A. Simionovici, M.D. Ynsa, E. Gontier, M. Heiss, T. Pouthier, A. Boudou, F. Rebillat, Nucl. Instr. and Meth. B 249 (2006) 653.
[19] T. Reinert, U. Reibetanz, M. Schwertner, J. Vogt, T. Butz, A. Sakellariou, Nucl. Instr. and Meth. B 188 (2002) 1.
[20] F. Watt, J.A. Van Kan, I. Rajta, A.A. Bettiol, T.F. Choo, M.B.H. Breese, T. Osipowicz, Nucl. Instr. and Meth. B 210 (2003) 14.
[21] <http://www.sales.hamamatsu.com/en/products/solid-state-division/si-photodiode-series/silicon-pin-photodiode/s1223.php>.
[22] J.A. van kan, A.A. Bettiol, F. Watt, F. Mater, Res. Soc. Symp. Proc. (2003) 777, T2.1.1.
[23] J.F. Ziegler, The Stopping and Range of Ions in Matter, Vols. 2–6, Pergamon Press, 1977. <http://www.srim.org/>.
[24] Oxford Microbeams Ltd., <http://www.microbeams.co.uk>.
[25] F. Zhang, J.A. van Kan, S.Y. Chiam, F. Watt, Nucl. Instr. and Meth. B, these Proceedings, doi:10.1016/j.nimb.2007.02.065.
[26] A. Simon, G. Kalinka, M. Jakšić, Ž. Pastuović, M. Novák, Á. Z Kiss, these Proceedings, doi:10.1016/j.nimb.2007.02.038.
[27] A. Simon, G. Kalinka, Nucl. Instr. and Meth. B 231 (2005) 507.
[28] H.J. Whitlow, S.J. Roosendaal, M. El Bouanani, R. Ghetti, P.N. Johnston, B. Jakobsson, R. Hellborg, H. Petersson, P. Omling, Z.G. Wang, Nucl. Instr. and Meth. B 135 (1–4) (1998) 523.
[29] R. Schwarz, M. Vieira, F. Macarico, S. Koynov, S. Cardoso, J.C. Soares, Defects in Semiconductors – ICDS-19, PTS 1-3 Materials Science Forum 258 (2) (1997) 593, Part 1–3.
[30] P. Aguer, L.C. Alves, Ph. Barberet, E. Gontier, S. Incerti, C. Michelet-Habchi, Zs. Kerte'sz, A.Z. Kiss, P. Moretto, J. Pallon, T. Pinheiro, J.E. Surle'ye-Bazeille, Z. Szikszai, A. Verı'ssimo, M.D. Ynsa, Nucl. Instr. and Meth. B 231 (2005) 292.
[31] Mischa Maetz, Wojtek J. Przybylowicz, Jolanda Mesjasz-Przybylowicz, Arthur Schûler, Kurt Traxel, Nucl. Instr. and Meth. B 158 (1999) 292.